Acta Cryst. (1979). A35, 319–325

The Theoretical Deformation Density for Oxalic Acid

BY HELGE JOHANSEN

Department of Chemical Physics, The Technical University of Denmark, DTH 301, *DK*-2800 *Lyngby, Denmark*

(*Received* 14 *June* 1978; *accepted* 20 *September* 1978)

Abstract

Theoretical deformation densities for oxalic acid and oxalic acid dihydrate have been determined by *ab initio* Hartree–Fock calculations using extended atomic basis sets. The results are in good agreement with experimental $X-N$ maps. The non-sphericity of the deformation density in certain bond cross sections has been established. Special emphasis is placed on the discussion of lone pairs and hydrogen bonds. The deformation density for the hydrate water has been analyzed.

Introduction

Electron density determinations are becoming more and more accurate, and this applies equally well to those obtained by experimental measurements as to those obtained from theoretical calculations. A good qualitative correspondence between calculated and experimental deformation densities has so far been established. The deformation density is here defined as the difference between the electron density of the system considered and the sum of the spherically averaged densities of the constituent atoms. However, the quantitative results differ considerably, and additional data are needed before more definite conclusions can be arrived at.

Oxalic acid has been selected by various research groups for detailed investigations in order to compare experiment with experiment, experiment with theory and theory with theory. By focusing on a single system, it is the general hope that more knowledge about the accuracies of the various methods will be obtained, and that the experimental and theoretical results will be able to be placed on an equal footing.

The general problem is well documented in the literature [see, for example, the reviews by Coppens & Stevens (1977) and Smith (1977)] and will not be discussed further here.

Oxalic acid exemplifies several chemically interesting concepts, such as single bonds, double bonds, hydrogen bonds, σ lone pairs and π lone pairs. As a test molecule it also has certain advantages in the technical aspects of both the experimental and theoretical analyses. From the latter point of view, it is a reasonably small molecule, it has some symmetry, and there is relatively little charge transfer between the molecules in the crystal (see below) – all properties which make the system tractable for calculation.

In the gas phase oxalic acid has an internal hydrogen bond (Náhlovská, Náhlovský & Strand, 1970), and as a solid the dihydrate crystallizes in two modifications, the so-called α and β forms, which differ mainly in the way the water and oxalic acid molecules are bridged with hydrogen bonds (Coppens & Sabine, 1969). The present investigation is, therefore, concerned with four different calculations: oxalic acid with and without the internal hydrogen bond (systems *A* and *B* respectively), and the α and β forms of oxalic acid dihydrate (systems *C* and *D*). The calculations for *A* and *B* have been performed with an extended basis set using polarization functions on all atomic centers, whereas a smaller basis set with polarization functions on the H atoms only was adopted for *C* and *D* in the calculations on the somewhat larger and less symmetrical dihydrates.

By calculating deformation densities for these four systems in selected planes, it is the aim of this study to obtain greater insight into the characteristics of the various bonds and lone pairs, as well as to obtain further and more accurate information for the comparison of theoretical and experimental deformation densities.

Details of calculations

The calculations in this study are of *ab initio* LCAO–SCF–MO (linear combination of atomic orbitals–self-consistent field–molecular orbital) type using the Hartree–Fock–Roothaan formalism (Roothaan, 1951). The basis sets used consisted of contracted Gaussian-type functions. For the calculations of oxalic acid alone, a primitive basis set of the form (C/11,6,1) (O/11,6,1) (H/6,1) was chosen (Duijneveldt, 1971), where the notation $(X/s,p,d)$ indicates the number of primitive *s*, *p* and *d* type sets of Cartesian Gaussians on the atom *X*. The functions were contracted (see, for example, Schaefer, 1972) to $\langle$C/5,3,1$\rangle$ $\langle$O/5,3,1$\rangle$ and $\langle$H/3,1$\rangle$, where the notation inside angle brackets is the same as above. The basis set is thus very similar to

0567-7394/79/020319-07$01.00

that used by Ermler, Mulliken & Clementi (1976) for the benzene molecule.

The dihydrate calculations were performed with a somewhat smaller basis set: (C/9,5) (O/9,5) (H/4,1), contracted to ⟨C/4,2⟩ ⟨O/4,2⟩ ⟨H/2,1⟩ (Duijneveldt, 1971). Because of the reduction in flexibility of the hydrogen basis set, the *s*-orbital exponents were scaled by a factor 1·3, which is known to give a more realistic description of this atom in a bonded situation.

The polarization functions used were those of Roos & Siegbahn (1970), with C and O *d* exponents of 0·63 and 1·33, respectively, and a H *p* exponent of 0·8.

For the geometrical parameters of the $(COO)_2$ section in all four systems, the results from the neutron diffraction study of α-deuterooxalic acid (α-DOX) (Coppens & Sabine, 1969) were chosen. The geometry for this section was fixed in order to facilitate the comparisons as well as the computations. The α-DOX coordinates were further used for the H positions in system *A* (Table 1) and for the positions of the water molecules in *C*. For calculation *B*, the gas-phase geometry with the internal hydrogen bond, the O–H distance of 1·056 Å and the C–O–H angle of 104·4° found by Náhlovská, Náhlovský & Strand (1970) were used. In the last calculation, system *D*, the water molecules were placed according to the neutron diffraction determination of the β form (Coppens & Sabine, 1969). The actual coordinates used are listed in Table 1; the $(COOH)_2$ section is taken to be planar with C_{2h} symmetry in all cases, whereas the water molecules in the dihydrates lower the symmetry to C_i for systems *C* and *D*.

Table 1. *Coordinates for the four calculations (in atomic units of length,* $a_0 = 0{\cdot}529166$ Å)

The numbers are experimentally significant to at most three places after the decimal point. *A*: oxalic acid from α-DOX geometry; *B*: hydrogen from gas-phase geometry; *C*: water from α-DOX geometry; *D*: water from β-DOX geometry. Atoms with indices 2 are generated by inversion symmetry.

System		*x*	*y*	*z*
A	C(1)	1·454175	0	0
	O(*A*1)	2·375989	−2·258835	0
	H(*A*1)	4·324230	−2·279238	0
	O(*B*1)	2·636747	1·952658	0
B	H(*A*1)	0·773891	−3·448658	0
C	O(*C*1)	7·140235	−2·397380	0·047609
	H(*B*1)	7·787140	−3·698591	1·117625
	H(*C*1)	8·055272	−2·537524	−1·498403
D	O(*C*1)	7·176776	−2·495550	0·250791
	H(*B*1)	8·427877	−2·926099	−0·947113
	H(*C*1)	7·965162	−2·232781	1·836664

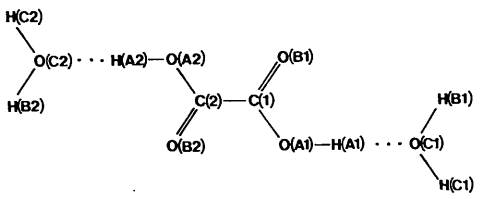

Fig. 1. Oxalic acid dihydrate: atomic labels.

For the molecular-orbital calculations, the joint *MOLECULE–ALCHEMY* program system (Almlöf, 1973; Bagus, 1972) was used.

The deformation density was calculated as the difference between the density of the system in question and a superposition of spherically averaged densities for the constituent atoms calculated with the same contracted Gaussian basis set (apart from the polarization functions). Electron density contours have been drawn for selected planes. The contour values are, however, not equidistant, as is prevalent for experimental studies; instead, there is a factor of two between adjacent levels. This logarithmic scale will enhance the small features and compress the larger ones, so that they can both be visible in the same picture. The units used are e a_0^{-3} ($1a_0 = 0{\cdot}529166$ Å), and the lowest numerical value for the positive (fully drawn) and negative (dashed) contours is 0·0025 e a_0^{-3}, corresponding to 0·017 e $Å^{-3}$. The typical first contour, 0·05 e $Å^{-3}$, of an experimental map is found between the second and third contours of the present investigations. The maps have been drawn without any thermal smearing.

Because of the program systems used, the atomic labelling (Fig. 1) is slightly at variance with the standard notation. The letters (*A*, *B* and *C*) label non-equivalent centers for a particular type of atom, and the numerals number the centers related by inversion symmetry. A notation as O(C2), or OC2 in the maps, therefore corresponds to $O(3^{ii})$.

Results and discussion

Total energies and orbital energies

The calculations are not intended for publication elsewhere, and a few values concerning the energies of the systems will, therefore, be given here. The total energies for the systems *A* and *B* are −376·4864 and −376·4845 a.u., respectively (1 atomic unit for energy, a.u., is $4{\cdot}3594 \times 10^{-18}$ J), but since the geometries have not been relaxed, the difference between the two is not physically significant.

Orbital energies for system *A* are listed in Table 2, and a comparison with the photoelectron spectrum (Meeks, Arnett, Larson & McGlynn, 1975; McGlynn & Meeks, 1976) is given in Table 3 [the validity of Koopmans's (1933) theorem being assumed]. The theoretical results have been shifted 1·23 eV in order to match the first experimental band. The agreement is fair, and one should not expect anything more, in spite of the large basis set, since effects from electron relaxation and electron correlation have not been taken into account. The molecular orbitals resulting from the

calculations are very delocalized, and no attempt has, therefore, been made to interpret the levels more than in terms of their symmetries in the point group C_{2h}. The conclusion from the experimental study, that the region 12–14 eV contains three bands (rather than two as the distinct peaks might suggest), is supported by the present calculation.

Deformation density for $(COOH)_2$

The theoretical deformation density for oxalic acid (system *A*) is shown in Fig. 2. The molecular plane and a plane $1a_0$ above have been depicted. The maxima for the radial charge distributions of $2p$ orbitals for C and O are located at about $1a_0$, so the second plane displays features which to a large extent are due to the π orbitals. The contours in the first plane show charge increase in all the σ bonds, in the two σ lone pairs of each O(*B*) atom, and in the σ lone pairs of the O(*A*) atoms. There is decrease of density in regions around the molecule, and the H atoms are situated in deformation density nodes. The second plane shows the carbonyl π bond, the O(*A*) π lone pair, the tops of the O(*B*) σ lone pairs and a tendency towards an increase of density in the π region of the C–C bond.

Table 2. *Orbital energies for oxalic acid (system A) in atomic units* (1 a.u. = $4{\cdot}3594 \times 10^{-18}$ J) (*point group* C_{2h})

Orbital	a_g	b_g	a_u	b_u
1	−20·6459	−0·6413	−0·6914	−20·6459
2	−20·5728	−0·5009	−0·5013	−20·5728
3	−11·4190			−11·4184
4	−1·5184			−1·4896
5	−1·3819			−1·3987
6	−0·9768			−0·8610
7	−0·7626			−0·7259
8	−0·7161			−0·6468
9	−0·5878			−0·5320
10	−0·4568			

Table 3. *Assignment of the photoelectron spectrum of oxalic acid (system A)*

Energies are in electron volts (1 eV = $1{\cdot}6021 \times 10^{-19}$ J). The calculated spectrum has been shifted 1·23 eV in order to match the first experimental band.

Orbital	Calculated	Experimental*
$10\,a_g$	11·20	11·20
$2\,b_g$	12·40	12·81
$2\,a_u$	12·41	13·25
$9\,b_u$	13·25	~13·25
$9\,a_g$	14·76	14·40
$1\,b_g$	16·22	15·59
$8\,b_u$	16·37	16·62
$1\,a_u$	17·58	17·3
$8\,a_g$	18·26	18·4

* Meeks, Arnett, Larson & McGlynn (1975); McGlynn & Meeks (1976).

The *X–N* experimental deformation density for α-deuterooxalic acid has been determined by Coppens, Sabine, Delaplane & Ibers (1969) using room-temperature data. A very good qualitative correspondence between Fig. 2(*a*) and the experimental results in Fig. 1(*b*) of the above reference is evident. The lone-pair regions and the bond regions look very similar and so does the node structure at the H position. Most of the features are also found in the room-temperature study of $(CH_3)_2NH_2HC_2O_4$ by Thomas (1977, Fig. 2), but the peaks are much more pronounced.

Of course the quantitative results differ substantially, since the theoretical densities have not been thermally smeared for comparison, but the scale in the theoretical

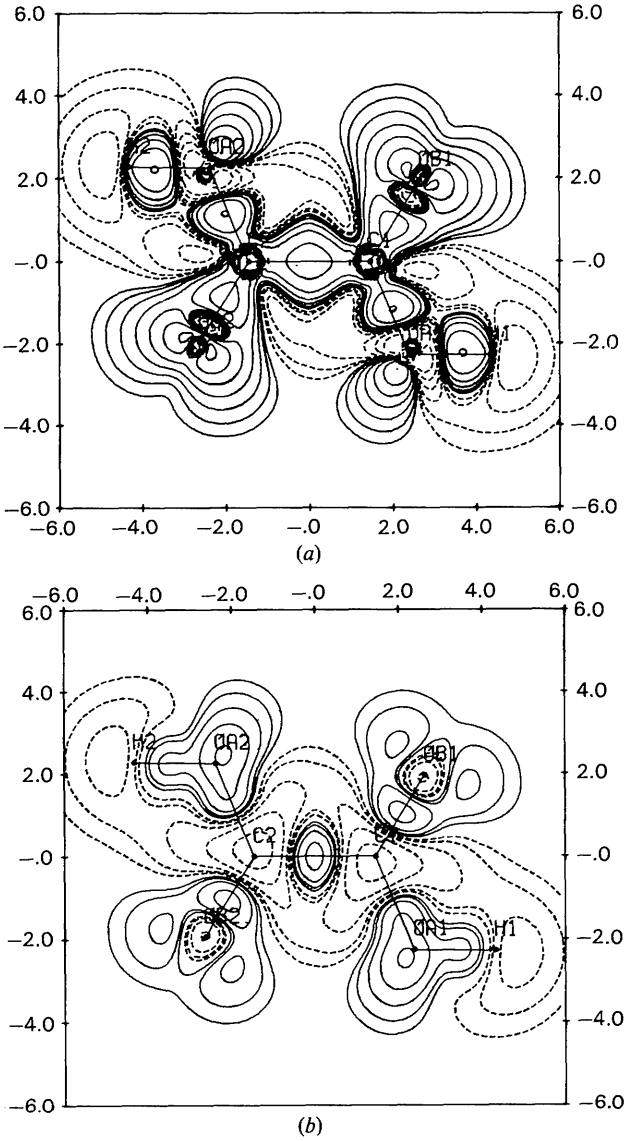

Fig. 2. Deformation density for oxalic acid (system *A*) (*a*) in the plane of the molecule and (*b*) $1a_0$ above. First contours are $\pm 0{\cdot}0025$ e a_0^{-3}; neighbouring contours differ by a factor of 2 (see text).

presentations, somewhat deceptively, makes up for part of the discrepancy. Fig. 6 of Thomas (1977) is an *X–N* map corrected for thermal smearing, and this map is, of course, much more in accord with the results of the present investigation. The approximate values for some of the bond and lone-pair maxima are listed in Table 4. The correspondence with the uncorrected experimental values is, as expected, poor, and the two experimental studies also differ appreciably. The trends are, however, reproduced. When the experimental results are corrected for thermal smearing the correspondence is also quantitatively in accord for many of the features. The thermal motion is thus responsible for most of the differences between the experimental and theoretical maps. Since sharp features will be more sensitive to thermal smearing (Coppens, 1974), the lone-pair regions differ the most. They will, like the *d*-orbital lobes in transition-metal complexes (Johansen, 1976), usually have higher values in theoretical investigations.

Bond cross sections

The deformation densities for the bond-midpoint cross sections of the C—C, C—O and C=O bonds have been given by Coppens, Sabine, Delaplane & Ibers (1969, Fig. 4). Non-sphericity was encountered for all three bonds, and π character was, therefore, ascribed to both the C—C and the C—O bonds. Corresponding theoretical maps are reported in Figs. 3 and 4(*b*). These figures also show elongations perpendicular to the molecular plane, and the ratios between vertical and horizontal diameters for the lowest positive contour are 1·26, 1·35 and 1·40 for C—C, C—O and C=O respectively. Also, the deficiency regions around the bonds are very similar in the two investigations. The non-sphericity of the C—C bond has also been demonstrated for $NaHC_2O_4.H_2O$ by Tellgren, Thomas & Olovsson (1977).

The C—O bond has been cut by three further planes in order to study the π lone-pair formation (Fig. 4). In particular, Fig. 4(*c*), which shows a plane one quarter of the bond away from the O atom, illustrates this nicely.

The hydrogen bonds

The gas-phase molecule (system *B*) has an internal hydrogen bond, but the deformation density (Fig. 5) is, apart from the change in geometry, almost identical with that for system *A* (Fig. 2). A hydrogen bond, therefore, does not give rise to any appreciable change in the deformation density. Rather, it originates from a more direct electrostatic attraction.

Table 4. *Approximate deformation density maxima* (e Å^{-3})

A comparison of two experimental investigations with the present theoretical results is given. The second column of the results of Thomas shows densities which are corrected for thermal smearing.

	Coppens *et al.*[a]	Thomas[b] Uncorrected	Thomas[b] Corrected	Present work
C—C	0·3	0·4	0·8	0·77
C—O(*A*)	0·2	0·3	0·7	0·55
C=O(*B*)	0·2	0·4	0·8	0·72
O(*A*)—H(*A*)	0·1	0·1	0·1	0·55
O(*C*)—H(*C*)	0·	0·2[c]	–	0·66
O(*A*) lone pair[d]	0·2	0·3	0·5	1·08
O(*B*) lone pair	0·2	0·3	0·7	1·28
O(*C*) lone pair[e]	0·2	0·2[c]	–	0·73

(*a*) Coppens, Sabine, Delaplane & Ibers (1969): Figs. 1(*b*) and 3.
(*b*) Thomas (1977): Figs. 3(*d*) and 6(*c*); results for $(CH_3)_2NH_2HC_2O_4$.
(*c*) Tellgren, Thomas & Olovsson (1977): Fig. 5; results for $NaHC_2O_4.H_2O$.
(*d*) In the $(COOH)_2$ plane (not maximum).
(*e*) In the H_2O plane (not maximum).

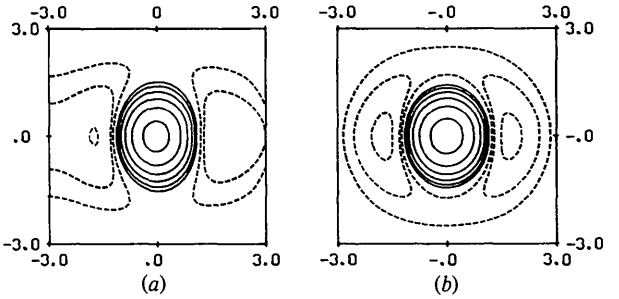

Fig. 3. Deformation density for oxalic acid (system *A*). Cross-sections perpendicular to and through the midpoints of (*a*) the C—C and (*b*) the C=O bonds. Contours are as in Fig. 2.

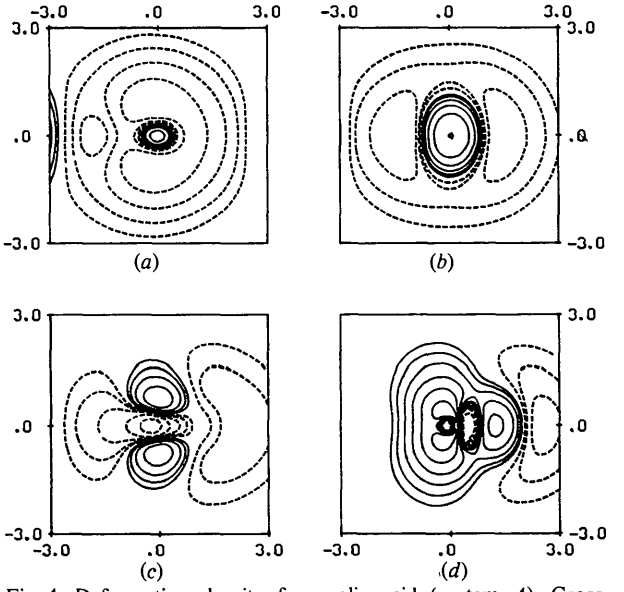

Fig. 4. Deformation density for oxalic acid (system *A*). Cross-sections through C—O perpendicular to the bond. Planes (*a*)–(*d*) are at the fractions $\frac{1}{4}$, $\frac{1}{2}$, $\frac{3}{4}$ and $\frac{1}{1}$ of the C—O bond measured from C. Contours are as in Fig. 2.

To illustrate the charge distribution in oxalic acid, gross charges and overlap populations have been listed for system *A* (Table 5). The H atom is found to be rather positive with a charge of +0·34 e, and the carbonyl O has a charge of −0·37 e. These figures change to +0·35 and −0·41 e, respectively, with the gas-phase geometry and thus tend towards greater polarization and stronger ionic attraction. In agreement with the density maps, the changes are, however, fairly small.

In the dihydrate, there are external hydrogen bonds to the water molecules. Systems *C* and *D* correspond to the α and β forms respectively (Coppens & Sabine, 1969). The two forms differ mainly with respect to the position of water relative to the oxalic acid molecule. In the β form, the three H atoms H(*A*), H(*B*), and H(*C*) (Fig. 1) have an almost planar arrangement with respect to O(*C*), whereas this atom has a more tetrahedral coordination in the α form. The deformation density for the O(*A*)–H(*A*)···O(*C*) hydrogen bond is depicted in Fig. 6 for both structures. The α form has an O(*C*) lone pair directed towards H(*A*), whereas the hydrogen bond in the β form is directed between the two lone pairs. This thus supports the conclusions reached by Coppens & Sabine (1969) from the structure determinations.

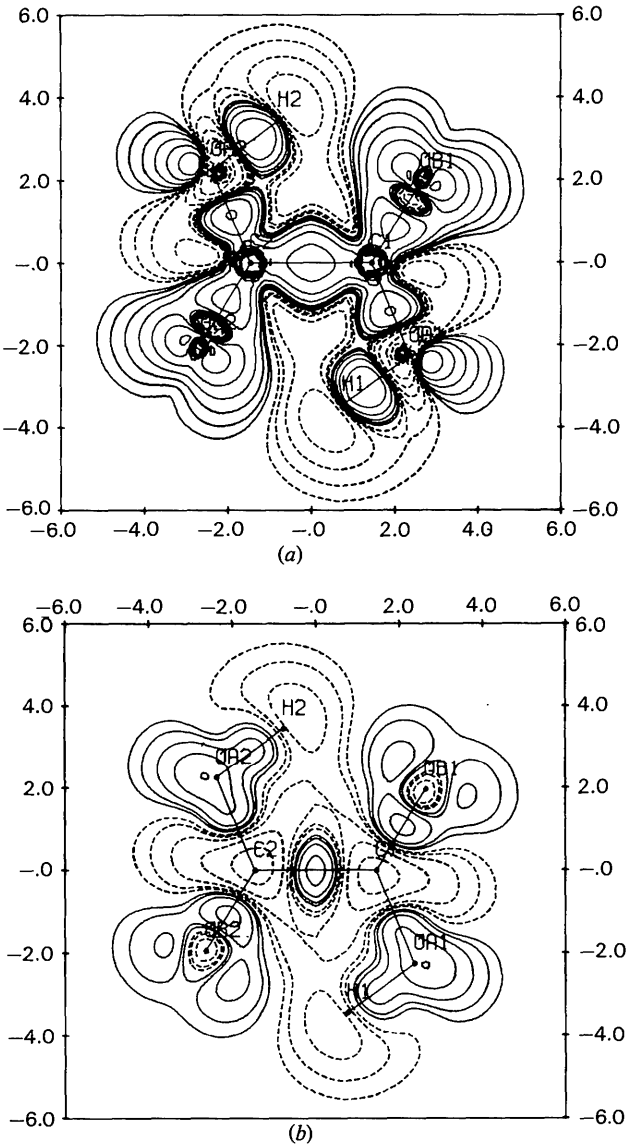

Fig. 5. Deformation density for oxalic acid in the gas-phase geometry (system *B*). Planes and contours are as in Fig. 2.

Table 5. *Gross charges and overlap populations for oxalic acid (system A)*

	Gross charge		Overlap population
C	+0·36 e	C–C	0·37
O(*A*)	−0·33	C–O(*A*)	0·67
O(*B*)	−0·37	C=O(*B*)	1·16
H(*A*)	+0·34	O(*A*)–H(*A*)	0·62

The H(*A*)···O(*C*) hydrogen bond is relatively short in both forms (1·493 and 1·520 Å respectively), and the H_2O molecule is probably dominated by this interaction. There are, however, additional hydrogen bonds which involve the water H atoms, and their effects have not been taken into account here.

As in the systems *A* and *B* (Figs. 2 and 5), the H atom is placed on a nodal structure of the deformation density. The negative area behind H(*A*) is somewhat compressed, but the general features are the same. There is, as in system *B*, no tendency towards a density increase on the H(*A*)···O(*C*) bond as such. If, on the other hand, the constituent molecules [$(COOH)_2$ + $2H_2O$] are used as reference systems instead of the spherical atoms (Fig. 7), an electron density increase is found for both the O(*A*)–H(*A*) and the H(*A*)···O(*C*) bonds, and there is a deficiency at the H position. The density increase on the hydrogen bond is, however, very small and may not be significant. In the O(*A*) and H(*A*) region the difference density is quite similar to the corresponding density in the water dimer (Smith, 1977, Fig. 3); this, however, is not the case in the O(*C*)

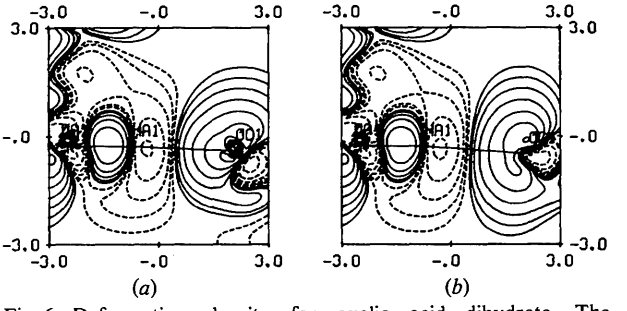

Fig. 6. Deformation density for oxalic acid dihydrate. The O(*A*)–H(*A*)···O(*C*) part has been depicted in the oxalic acid plane. (*a*) System *C*, (*b*) System D. Contours are as in Fig. 2.

region. An experimental determination for the N—H···O hydrogen bond in α-glycine has been given in Fig. 4 of Almlöf, Kvick & Thomas (1973). The features there are very similar to those in oxalic acid dihydrate, and thus support a cautious generalization to other hydrogen-bonded systems.

The water molecules

The deformation density for H_2O has been depicted in the molecular plane for systems *C* and *D* (Fig. 8). Apart from the geometrical differences the features are very similar. The plane in Fig. 8(*b*) passes almost through H(*A*), and the figure, therefore, complements Fig. 6(*b*) and gives further support to the conclusion that the hydrogen bond is in a direction between two O lone pairs.

The maps are, however, somewhat at variance with the experimental results (Fig. 3 of Coppens, Sabine, Delaplane & Ibers, 1969). The general features may be recognized, but the water molecule is much more electron deficient in the experimental study. A similar result was found for the water molecule in $LiHCOO.H_2O$ in a study by Thomas, Tellgren & Almlöf (1975, Fig. 3). It is, of course, reasonable to assume that a certain charge transfer takes place, and Coppens & Stevens (1977) report that a typical experimental value is 0·2 e for one water molecule. The present calculations show a transfer of 0·08 e, and, since only the short hydrogen bond has been taken into account, this value is too low, but it is questionable whether this limitation is able to explain the discrepancy. The experimental study of $NaHC_2O_4.H_2O$ by Tellgren, Thomas & Olovsson (1977, Fig. 5) is much more in accord with the maps in Fig. 8, and a more accurate experimental determination of oxalic acid dihydrate therefore seems appropriate at this point.

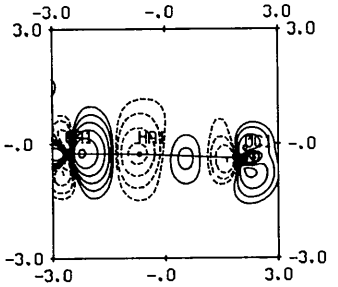

Fig. 7. Difference between the density of oxalic acid dihydrate (system *C*) and the sum of the densities for the constituent molecules [$(COOH)_2 + 2H_2O$]. The plane is as in Fig. 6 and the contours are as in Fig. 2.

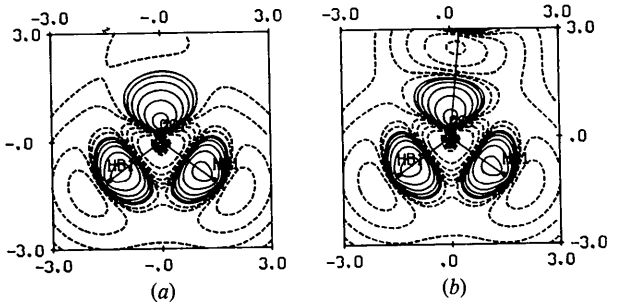

Fig. 8. Deformation density for oxalic acid dihydrate in the plane of a water molecule [H(*B*)—O(*C*)—H(*C*)]. (*a*) System *C*, (*b*) system *D*. Contours are as in Fig. 2.

Conclusions

It can be concluded that there is very good qualitative agreement between the experimental and theoretical deformation densities for oxalic acid, and that the main features correspond well to normal chemical concepts such as bonds and lone pairs. When thermal smearing is taken into account, the quantitative results are also in accord. The calculations have given further support to the non-sphericity of the C—C and C—O bonds, and thus for the assignment of a certain π character to these bonds.

It was found that the hydrogen bonds only indirectly modify the deformation density, their main effect being to adjust the positions of the lone pairs. The α and β forms of the dihydrate were found to have different forms of hydrogen bonds. In the α form the H atom from oxalic acid points towards a lone pair of the water O atom, whereas it is directed between two lone pairs in the β form.

The correspondence between theory and experiment is poorer for the water molecules. The discrepancy is probably due to inaccuracies both in the calculations, where only the strong hydrogen bond has been included and where the basis set has been restricted, and in the experiments, where water molecules are usually less accurately determined.

Professor Philip Coppens is gratefully thanked for fruitful discussions. The computations were performed at NEUCC, The Technical University of Denmark.

References

ALMLÖF, J. (1973). *Proceedings of the Second Seminar on Computational Problems in Quantum Chemistry, Strassburg* 1972, pp. 14–25. Munich: Max-Planck-Institut.

ALMLÖF, J., KVICK, Å, & THOMAS, J. O. (1973). *J. Chem. Phys.* **59**, 3901–3906.

BAGUS, P. S. (1972). *Documentation for ALCHEMY*. IBM Res. Rep. RJ1077.

COPPENS, P. (1974). *Acta Cryst.* B**30**, 255–261.

COPPENS, P. & SABINE, T. M. (1969). *Acta Cryst.* B**25**, 2442–2451.

COPPENS, P., SABINE, T. M., DELAPLANE, R. G. & IBERS, J. A. (1969). *Acta Cryst.* B**25**, 2451–2458.

COPPENS, P. & STEVENS, E. D. (1977). *Adv. Quantum Chem.* **10**, 1–35.
DUIJNEVELDT, F. B. VAN (1971). IBM Res. Rep. RJ945.
ERMLER, W. C., MULLIKEN, R. S. & CLEMENTI, E. (1976). *J. Am. Chem. Soc.* **98**, 388–394.
JOHANSEN, H. (1976). *Acta Cryst.* A**32**, 353–355.
KOOPMANS, T. (1933). *Physica*, **1**, 104–113.
MCGLYNN, S. P. & MEEKS, J. L. (1976). *J. Electron Spectrosc. Relat. Phenom.* **8**, 85–93.
MEEKS, J. L., ARNETT, J. F., LARSON, D. B. & MCGLYNN, S. P. (1975). *J. Am. Chem. Soc.* **97**, 3905–3908.
NÁHLOVSKÁ, Z., NÁHLOVSKÝ, B. & STRAND, T. G. (1970). *Acta Chem. Scand.* **24**, 2617–2628.
ROOS, B. & SIEGBAHN, P. (1970). *Theor. Chim. Acta*, **17**, 199–208.
ROOTHAAN, C. C. J. (1951). *Rev. Mod. Phys.* **23**, 69–89.
SCHAEFER, H. F. (1972). *The Electronic Structure of Atoms and Molecules: A Survey of Rigorous Quantum Mechanical Results*. Reading, Mass.: Addison–Wesley.
SMITH, V. H. JR (1977). *Phys. Scr.* **15**, 147–162.
TELLGREN, R., THOMAS, J. O. & OLOVSSON, I. (1977). *Acta Cryst.* B**33**, 3500–3504.
THOMAS, J. O. (1977). *Acta Cryst.* B**33**, 2867–2876.
THOMAS, J. O., TELLGREN, R. & ALMLÖF, J. (1975). *Acta Cryst.* B**31**, 1946–1955.

Acta Cryst. (1979). A**35**, 325–327

On Antisymmetric Atomic Vibrations in Zinc

BY M. MERISALO

Department of Physics, University of Helsinki, SF-00170 Helsinki 17, Finland

AND F. K. LARSEN

Department of Inorganic Chemistry, University of Aarhus, DK-8000 Aarhus C, Denmark

(*Received* 20 *September* 1978; *accepted* 1 *November* 1978)

Abstract

Recent elastic neutron scattering data [Merisalo & Larsen (1977). *Acta Cryst.* A**33**, 351–354] have been reconsidered. A significant value for the cubic anharmonic force constant $\alpha_{33} = -1{\cdot}80\,(30) \times 10^{-19}$ J Å^{-3} of the one-particle potential was obtained, and is compared with other recent determinations.

In a previous paper (Merisalo & Larsen, 1977; hereinafter referred to as paper I) we reported the results and analysis of a neutron single-crystal diffraction study of Zn at 300 K. The data, interpreted in the framework of the effective one-particle potential approximation, showed significant quartic terms in the anharmonic potential, whereas the value of the cubic (antisymmetric) anharmonic parameter α_{33} representing deviations from axial symmetry in the initial analysis did not differ significantly from zero and was consequently ignored in the final refinement.

Recently, a non-zero value for α_{33} was determined by an X-ray measurement of almost-forbidden reflexions 301 and 303 (Merisalo, Järvinen & Kurittu, 1978). It was therefore considered desirable to reassess the validity of the assumption $\alpha_{33} = 0$ made in our neutron data analysis. In this paper we shall also discuss correlations between the various parameters and describe qualitatively the atomic thermal motion in the anharmonic approximation.

Each unit cell of h.c.p. Zn contains two atoms, A and B, at the special positions $\pm(\frac{1}{3},\frac{2}{3},\frac{1}{4})$. The origin, taken midway between these two points, is an inversion centre. A basal projection of the atomic arrangement and the definition of the atomic Cartesian coordinate system xyz (x axis along 2, y axis perpendicular to m, z-axis along $\bar{6}$) is shown in Fig. 1. The exact expression for the structure amplitudes $F(\mathbf{Q})$ becomes

$$F(\mathbf{Q}) = 2b\left[T_{s,A}(\mathbf{Q})\cos 2\pi\left(\frac{h+2k}{3}+\frac{l}{4}\right) - T_{a,A}(\mathbf{Q})\sin 2\pi\left(\frac{h+2k}{3}+\frac{l}{4}\right)\right],$$

where $T_{s,A}(\mathbf{Q})$ and $T_{a,A}(\mathbf{Q})$ are the symmetric and antisymmetric (*i.e.* real and imaginary) parts of the atomic temperature factor $T(\mathbf{Q})$ given in paper I, $\mathbf{Q}$ is the diffraction vector, and b is the scattering length. This expression was used for the calculated structure amplitudes in refining the potential parameters by a least-squares method. Refinements were made applying model 2 of paper I in which the harmonic parameters were kept fixed at the values determined from the

0567-7394/79/020325-03$01.00